JOURNAL OF VIROLOGY, Sept. 2008, p. 8487–8499 Vol. 82, No. 17
0022-538X/08/$08.00+0 doi:10.1128/JVI.00851-08

Targeting the Apoptotic Pathway with BCL-2 Inhibitors Sensitizes Primary Chronic Lymphocytic Leukemia Cells to Vesicular Stomatitis Virus-Induced Oncolysis▽

Vanessa Fonseca Tumilasci,[1,2] Stephanie Olière,[1,2]† Thi Lien-Ahn Nguyên,[1,2]† April Shamy,[3] John Bell,[4] and John Hiscott[1,2,3]*

Molecular Oncology Group, Lady Davis Institute–Jewish General Hospital,[1] and Department of Microbiology and Immunology, McGill University,[2] Montreal, Quebec H3T 1E2, Canada; Department of Medicine, Jewish General Hospital, McGill University, Montreal, Quebec H3T 1E2, Canada[3]; and Ottawa Health Research Institute, University of Ottawa, Ottawa, Ontario K1Y 4E9, Canada[4]

Received 22 April 2008/Accepted 17 June 2008

Chronic lymphocytic leukemia (CLL) is characterized by clonal accumulation of $CD5^+$ $CD19^+$ B lymphocytes that are arrested in the G_0/G_1 phase of the cell cycle and fail to undergo apoptosis because of overexpression of the antiapoptotic B-cell CLL/lymphoma 2 (BCL-2) protein. Oncolytic viruses, such as vesicular stomatitis virus (VSV), have emerged as potential anticancer agents that selectively target and kill malignant cells via the intrinsic mitochondrial pathway. Although primary CLL cells are largely resistant to VSV oncolysis, we postulated that targeting the apoptotic pathway via inhibition of BCL-2 may sensitize CLL cells to VSV oncolysis. In the present study, we examined the capacity of EM20-25—a small-molecule antagonist of the BCL-2 protein—to overcome CLL resistance to VSV oncolysis. We demonstrate a synergistic effect of the two agents in primary ex vivo CLL cells (combination index of 0.5; $P < 0.0001$). In a direct comparison of peripheral blood mononuclear cells from healthy volunteers with primary CLL, the two agents combined showed a therapeutic index of 19-fold; furthermore, the combination of VSV and EM20-25 increased apoptotic cell death in Karpas-422 and Granta-519 B-lymphoma cell lines ($P < 0.005$) via the intrinsic mitochondrial pathway. Mechanistically, EM20-25 blocked the ability of the BCL-2 protein to dimerize with proapoptotic BAX protein, thus sensitizing CLL to VSV oncolytic stress. Together, these data indicate that the use of BCL-2 inhibitors may improve VSV oncolysis in treatment-resistant hematological malignancies, such as CLL, with characterized defects in the apoptotic response.

Chronic lymphocytic leukemia (CLL) is one of the most common leukemias in the Western hemisphere, accounting for up to 30% of all diagnosed leukemias. CLL is characterized by a progressive accumulation of a monoclonal $CD5^+$ $CD19^+$ B-lymphocyte population in the peripheral blood, bone marrow, and lymphoid organs as well as low levels of cell surface immunoglobulin, and CLL cells ultimately acquire an aggressive and lethal phenotype (12). Malignant B cells are arrested in G_0/G_1 phase of the cell cycle and fail to undergo apoptosis due to overexpression of B-cell CLL/lymphoma 2 (BCL-2) protein in malignant CLL cells (18, 51). The antiapoptotic BCL-2 protein plays a key role in the control of the intrinsic mitochondrial pathway and promotes cell survival by inhibiting the function of proapoptotic proteins, such as BAX and BAK (4, 39, 46). Although chromosomal translocation events, such as t(14:18), have been associated with BCL-2 overexpression in several types of follicular B-cell lymphomas, the mechanisms that mediate BCL-2 expression in CLL cells remain unclear (4, 26, 40). Despite advances in cancer therapeutics, CLL disease remains resistant to existing treatments; the majority of therapies are palliative, with only a small percentage of patients achieving a complete response (1, 2).

Viral oncolytic therapy, involving the use of replication-competent viruses that specifically target and kill cancer cells, while sparing normal tissues, is a promising new strategy for cancer treatment (32, 37). This selectivity is achieved by exploiting cell surface or intracellular aberrations in gene expression that arise during the development of malignancies and appear to favor cancer cell proliferation at the expense of the host antiviral program (reviewed in references 5, 37, and 41). Vesicular stomatitis virus (VSV) is an enveloped, single-stranded RNA virus and member of the *Rhabdoviridae* family possessing intrinsic oncolytic properties (37, 52, 53). Aspects of interferon signaling and the action of downstream effectors, including translational control, are compromised in malignant cells, thus affording a cellular environment that facilitates viral replication and cell killing—uninterrupted by the host antiviral response (58). Naturally attenuated VSV strains (termed AV1 and AV2) harboring mutations in the matrix protein have a potentially greater therapeutic margin compared to wild-type VSV (49), because these attenuated strains fail to block the nuclear to cytoplasmic transport of host mRNA, including interferon and cytokine mRNA, and therefore generate an antiviral response (20) that contributes to a strong protective effect in normal tissue.

It has been generally accepted that VSV induces apoptosis in a caspase-3- and caspase-9-dependent manner (22, 53). De-

* Corresponding author. Mailing address: Lady Davis Institute for Medical Research, 3755 Cote Ste. Catherine, Montreal, Quebec, Canada H3T 1E2. Phone: (514) 340-8222, ext. 5265. Fax: (514) 340-7576. E-mail: john.hiscott@mcgill.ca.

† These two authors contributed equally to this work.

▽ Published ahead of print on 25 June 2008.

TABLE 1. Characteristics of patients diagnosed with B-CLL

Patient	Age (yr)	Gender[a]	No. of WBC[b] (10^9/liter)	% positive cells		
				$CD5^+$	$CD19^+$	$CD5^+$ $CD19^+$
1	78	F	10.7	87	73	70
2	71	F	94.4	46	79	37
3	54	M	18.3	83	79	72
4	41	M	42.7	78	71	62
5	48	M	42	66	72	52
6	54	M	12.2	61	56	55
7	41	M	46.7	71	37	33
8	46	M	42.9	78	64	63
9	47	F	221	91	87	85
10	71	M	9.6	91	83	79
11	63	F	29	98	68	67
12	84	F	83.3	92	94	87
13	66	F	17.9	91	97	89
14	63	M	21.4	83	91	81
15	62	M	1.4	61	97	58

[a] F, female; M, male.
[b] WBC, white blood cells.

spite discrepancies about the particular involvement of either the intrinsic or extrinsic pathway in VSV-induced apoptosis (23, 24), the proapoptotic protein BAX represents the convergence point of VSV-mediated cell death, triggering mitochondrial membrane potential depolarization (50). We previously reported (11) that primary ex vivo CLL cells are resistant to VSV-induced apoptosis; given the importance of mitochondrial pathway in VSV oncolysis, we hypothesized that inhibition of BCL-2 function may restore activation of the intrinsic apoptotic pathway in VSV-infected malignant CLL cells. Indeed, we demonstrate that primary CLL cells that are refractory to VSV-induced apoptosis can be rendered sensitive to VSV oncolysis by combination treatment with VSV-AV1 and a BCL-2 inhibitor. Impressively, our data also demonstrate that induction of apoptosis by combination treatment is not toxic for normal peripheral blood marrow cells (PBMCs), suggesting that the use of VSV and a BCL-2 inhibitor constitutes a promising, therapeutic approach for the treatment of chronic lymphocytic leukemia.

MATERIALS AND METHODS

Patients and PBMC isolation. PBMCs were obtained from healthy individuals and CLL patients at the Jewish General Hospital, Montreal, Quebec, Canada, following written, informed consent, in agreement with the Jewish General Hospital and McGill University Research Ethics Committee. Blood mononuclear cells were isolated by centrifugation (400 × *g* at 20°C for 25 min) of blood samples on a Ficoll-Hypaque density gradient (GE Healthcare Bio-Sciences Inc., Oakville, Ontario, Canada). PBMCs were cultured in RPMI 1640 medium supplemented with 15% heat-inactivated fetal bovine serum (Wisent Inc., St-Bruno, Quebec, Canada) and 100 U of penicillin and streptomycin per ml. PBMCs were cultured at 37°C in a humidified, 5% CO_2 incubator.

CLL patients included in our study were selected on the basis of the patient's willingness to donate blood. Median age, sex, and absolute lymphocyte counts were typical of CLL patients in general. Patients were not on therapy at the time of analysis. We determined that only cells from patients with B-cell CLL (B-CLL) with malignant cells positive for both CD5 and CD19 markers would be used in this study (1, 2, 12). According to the National Cancer Institute-Sponsored Working Group guidelines for the diagnosis and criteria for response for CLL, as part of the diagnosis of B-CLL, >30% of all nucleated cells from the bone marrow must be lymphoid. In agreement, all PBMC cells from CLL patients, used in this study, expressed more than 30% malignant B cells (Table 1).

Cell lines. The human B-lymphoma cell lines (Granta-519 and Karpas-422) used in this study were purchased from the German Collection of Microorganisms and Cell Cultures and were grown in RPMI 1640 medium and Dulbecco's modified Eagle's medium (Wisent Inc.), respectively, supplemented with 10% fetal calf serum and with penicillin and streptomycin. All cells were maintained at 37°C and 5% CO_2. Wild-type and Bcl-2-expressing Jurkat T cells were maintained in RPMI 1640 medium (Wisent Inc.) supplemented with 10% fetal calf serum. The Bcl-2-expressing system was previously described and was a gift from R. Sekaly (University of Montreal, Montreal, Quebec, Canada) (7).

Virus production, quantification, and infection. Construction of VSV-AV1 and recombinant rVSV-Δ51-GFP (termed here VSV-AV1-GFP) was previously described (53). Virus stocks were grown in Vero cells (purchased from ATCC, Bethesda, MD), concentrated from cell-free supernatants, and titrated by standard plaque assay. Briefly, confluent monolayers of Vero cells in six-well plates were infected with 0.1 ml of serially diluted samples; after 1 h at 37°C, the medium was replaced with complete medium containing 0.5% methylcellulose (Sigma Aldrich, Oakville, Ontario, Canada) for 48 h. Vero cells were fixed in 4% formaldehyde and stained with crystal violet. Plaques were counted, and titers were calculated as PFU per milliliter. Duplicate experiments were performed, and the averages of the virus titers were calculated. VSV-AV1 was used for experiments with primary cells and for 5,5′,6,6′-tetrachloro-1,1′,3,3′-tetraethylbenzimidazolyl-carbocyanine iodide (JC-1) incorporation assay. Primary lymphocytes or lymphoma cell lines were infected with VSV at an multiplicity of infection (MOI) of 0.1 PFU/cell (Granta-519) or 10 PFU/cell (primary PBMCs and Karpas-422) for 1 h in serum-free medium at 37°C. The cells were then incubated with complete medium at 37°C for the indicated times.

Apoptotic response. EM20-25 [5-(6-chloro-2,4-dioxo-1,3,4,10-tetrahydro-2H-9-oxa-1,3-diaza-anthracen-10-yl)-pyrimidine-2,4,6-trione] (Calbiochem, San Diego, CA) was dissolved in dimethyl sulfoxide to a stock concentration of 1 mM, aliquoted, and stored at −20°C. EM20-25 (Calbiochem, San Diego, CA) was diluted in medium to a concentration of 10 μM. Cells were cultured at a density of 5×10^6 cells/ml. A fresh aliquot of EM20-25 was thawed for each experiment, and drug was added to the medium at the desired concentrations for 30 min prior to infection. After incubation with the inhibitor, cells were infected with VSV-AV1 or VSV-AV1-GFP (Δ51) at the MOIs described above. Mock-infected cells were used as a control. After incubation at 37°C in 5% CO_2 for 1 h, complete medium containing freshly thawed EM20-25 at 10 μM was added. Cells were incubated for periods of time varying from 6 h to 7 days and then analyzed for apoptosis by flow cytometry, Western blotting, and caspase activity and analyzed for virus replication by Western blotting, plaque assay, and reverse transcription-PCR (RT-PCR).

Flow cytometry. Total PBMCs were isolated as described above. Aliquots (0.5×10^6 to 1.0×10^6 cells) of cells treated or not with EM20-25 (10 μM) and infected or not with VSV-AV1 (MOI of 10) were washed with phosphate-buffered saline (PBS) and stained with fluorescein isothiocyanate-conjugated CD5, phycoerythrin-conjugated CD19 for 45 min on ice, and allophycocyanin (APC)-conjugated annexin V for 15 min in 1× annexin V binding buffer on ice. B-lymphoma cells Karpas-422 and Granta-519 were treated or not with EM20-25 (10 μM) and infected or not with VSV-AV1 (MOIs of 10 and 0.01); aliquots (0.5×10^6 to 1.0×10^6 cells) were washed with PBS and stained with APC-conjugated annexin V for 15 min in 1× annexin V binding buffer on ice. The percentage of apoptotic cells was measured in $CD5^+$ $CD19^+$ B-cell population. Flow cytometry (1×10^4 cells/measurement) was performed with a FACSCalibur (Becton-Dickinson, Mississauga, Ontario, Canada) and analyzed with CellQuest software and FCS Express version 3 (De Novo Software, Los Angeles, CA). All antibodies were purchased from BD Biosciences.

Semiquantitative RT-PCR. Total RNA was extracted from cells using RNase extraction kit (Qiagen, Mississauga, Ontario, Canada) according to the manufacturer's instructions. RT-PCR was performed using 0.3 μg of RNA resuspended in RNase-free double-distilled H_2O and oligo(dT_{12-18}) primer (Invitrogen Canada Inc., Burlington, Ontario, Canada) according to the manufacturer's instructions. RT was performed using Superscript II at 42°C for 1 h. Following the RT reactions, cDNA samples were brought to a final volume of 100 μl of which 5 μl was used as template for each PCR with *Taq* polymerase. The primer sequences used in this study for PCR were as follows: for M protein, forward (5′-GCGAAGGCAGGCCTTATTTG-3′) and reverse (5′-CTTTTTCTCGACA ATCAGGCC-3′). PCR fragments were amplified at an annealing temperature of 55°C for 35 cycles. Products were run on a 1% agarose gel, revealed through use of a Typhoon 9400 phosphorimager (GE Healthcare Bio-Sciences), and quantification was performed using ImageQuant 5.2 software (GE Healthcare Bio-Sciences Inc., Oakville, Ontario, Canada).

Protein extraction and Western blot analysis. Cells were washed twice with ice-cold PBS, and proteins were extracted in ice-cold lysis buffer containing PBS,

0.05% NP-40, 0.1% glycerol, 30 mM NaF, 40 mM β-glycerophosphate, 10 mM Na_3VO_4, and protease inhibitor cocktail (Sigma-Aldrich, Oakville, Ontario, Canada) at a dilution of 1/1,000. Extracts were kept on ice for 15 min and centrifuged at 10,000 × *g* for 25 min (4°C), and supernatants were stored at −80°C. Protein concentration was determined with Bio-Rad protein assay reagent (Bio-Rad, Hercules, CA). Mitochondrial versus cytosol fractions of cells were prepared using a mitochondria isolation kit for cultured cells (Pierce, Rockford, IL) according to the manufacturer's instructions. Protein extracts (30 μg) were resolved using 12 to 14% sodium dodecyl sulfate (SDS)-polyacrylamide gel electrophoresis and transferred to nitrocellulose membranes (Hybond C Super; GE Healthcare Bio-Sciences Inc.). The membranes were blocked for 1 h in 5% nonfat dried milk in Tris-buffered saline containing 0.5% Tween 20. The membranes were then incubated with any of the following primary antibodies: anti-rabbit VSV (1:5,000), anti-cleaved caspase-3 (Cell Signaling, Danvers, MA) (1:2,000), anti-rabbit β-actin (Cell Signaling, Danvers, MA) (1:1,000), or anti-mouse BCL-2 (Santa Cruz Biotechnology, Santa Cruz, CA) (1:2,000). The immunocomplexes were detected with horseradish peroxidase-conjugated secondary antibodies and enhanced chemiluminescence according to the manufacturer's specifications (ECL kit; GE Healthcare Bio-Sciences Inc.). Cytochrome *c* was analyzed with anti-rabbit cytochrome *c* monoclonal antibody (MAb) or control antibody anti-mouse β-actin (Cell Signaling, Danvers, MA). Western blot quantification was assessed by densitometric analyses of scanned films with the use of the Scion Image 4.0. software.

Coimmunoprecipitation assay. Cells were lysed with 1% CHAPS lysis buffer {10 mM HEPES (pH 7.4), 150 mM NaCl, 1% 3-[(3-cholamidopropyl)-dimethylammonio]-1-propanesulfonate (CHAPS)} containing protease inhibitors. Total protein (200 μg) was incubated with 2 μg of anti-BCL-2 MAb (Santa Cruz Biotechnology, Santa Cruz, CA) or 2 μg of anti-BAX MAb (clone 6A7) (Sigma Aldrich, Oakville, Ontario, Canada) in CHAPS lysis buffer at 4°C overnight on a rotator. Immunoprecipitates were collected by incubating with 20 μl protein L-agarose (Santa Cruz Biotechnology, Santa Cruz, CA) for 4 h at 4°C, followed by centrifugation for 1 min. The pellets were washed three times with CHAPS lysis buffer, and beads were boiled in 2× SDS buffer and analyzed by Western blotting using the anti-BAX MAb (Santa Cruz Biotechnology, Santa Cruz, CA).

Measurement of mitochondrial potential by JC-1 staining. Cells (0.5×10^6) were cultured in six-well plates. After treatment with EM20-25 and/or VSV-AV1, the cells were collected, washed in PBS, and resuspended in medium containing JC-1 (Molecular Probes-Invitrogen Canada Inc., Ontario, Canada) at a final concentration of 1 mM/liter and incubated at 37°C for 15 min. After incubation, cells were subjected to flow cytometry analysis on a FACSCalibur (Becton-Dickinson) and analyzed with CellQuest software.

Quantitative measurement of caspase activity. Cells were lysed in buffer containing 50 mM HEPES (pH 7.4), 100 mM NaCl, 0.1% CHAPS, 0.1 mM EDTA, and 1 mM dithiothreitol. The lysates were clarified by centrifugation, and the supernatants were used for enzyme assays. Enzymatic reactions were carried out in 2.5× piperazine-*N*,*N*′-bis(2-ethanesulfonic acid) (PIPES) buffer containing 20 μg of protein lysate and 5 μM Asp-Glu-Val-Asp (DEVD)–7-amino-4-trifluoromethyl coumarin (AFC) or 5 μM Leu-Glu-His-Asp (LEHD)-AFC (both from BioMol International, Plymouth Meeting, PA). Fluorescent AFC formation was measured at a excitation wavelength of 390 nm and emission wavelength of 538 nm for 30 cycles using a Bio-Rad Fluoromark.

Viability assay. Cell viability was assessed by 3-(4,5-dimethylthiazol)-2,5-diphenyl tetrazolium (MTT) dye absorbance according to the manufacturer's instructions (Chemicon International, Billerica, MA). Cells were seeded in 96-well plates at a density of 5×10^5 cells (PBMCs) per well or 100,000 cells per well (Karpas-422 and Granta-519 cells). For drug combination studies, cells were treated or not with EM20-25 (10 μg) and infected or not with VSV-AV1 (MOI of 10) where indicated. For 50% inhibitory concentration (IC_{50}) assay, increasing concentrations of EM20-25 (300 nm to 200 μM) were used. Plates were incubated at 37°C and 5% CO_2 for 7 days. Each experimental condition was tested in quadruplicate experiments.

Statistical, synergism, and therapeutic index analyses. The statistical analysis was performed using the Student's *t* test. *P* values that were <0.05 were considered statistically significant. Average values were expressed as means ± standard deviations (SDs). The following equation was used to determine the combined cytotoxic effects of EM20-25 according to the method of Chou and Talalay (15): CI¼[(*D*)1/(Dx)1]þ[(*D*)2/(Dx)2]þ(*D*)1(*D*)2/(Dx)1(Dx)2, where (*D*)1 and (*D*)2 are the doses of treatments 1 and 2 that produce the *x* effect when used in combination and (Dx)1 and (Dx)2 represent the doses of treatments 1 and 2 that produce the same *x* effect when used alone. The combination is additive when the CI equals 1.0, synergistic when the CI is <1.0, and antagonistic when the CI is >1.0. The therapeutic index is the capacity or propensity of a drug to affect one cell population in preference to others, i.e., the ability of a drug to affect one kind of cell and produce effects in doses lower than those required to affect other cells. The therapeutic index was calculated by measuring 50% lethal dose/50% therapeutically effective dose, where the lethal dose applies to the normal population and the therapeutically effective dose applies to the malignant population (14).

RESULTS

Primary CLL cells are resistant to VSV-AV1-induced apoptosis. Overexpression of the antiapoptotic BCL-2 protein has been associated with an apoptosis-resistant phenotype in CLL and other malignances (31, 40, 42). To analyze VSV-induced oncolysis in BCL-2-overexpressing malignant cells, primary CLL cells from seven patients were infected with a naturally attenuated variant of VSV (AV1) at an MOI of 10, and by 96 h postinfection, cells were analyzed for virus replication and apoptosis; all samples showed high levels of BCL-2 protein compared to samples from healthy volunteers (Fig. 1a). Despite the fact that viral replication was detected in all samples (Fig. 1c), VSV-AV1 did not induce significant apoptosis in the CLL samples assayed by annexin V staining (Fig. 1b). Indeed, infection at higher MOIs of VSV-AV1 (MOIs of 10, 30, and 60) did not further increase apoptosis (Fig. 1d and e), suggesting that BCL-2 overexpression may play a role in resistance to VSV-induced apoptosis in CLL cells.

BCL-2 inhibitor EM20-25 sensitizes ex vivo CLL cells to VSV-AV1 oncolysis. Small organic molecules, such as EM20-25 (36, 45) (Fig. 2a), have been shown to sensitize apoptosis-resistant cells to cytotoxic drugs by binding to BCL-2 and disrupting interactions with proapoptotic proteins, such as BAX and BAK. As such, investigations are under way to explore the use of small-molecule inhibitors as therapeutic agents for the treatment of malignancies that overexpress BCL-2 (33, 34, 59). To examine the effect of EM20-25 on VSV oncolysis in CLL cells, primary human CLL cells from seven different patients (CLL8 to CLL11 and CLL13 to CLL15) were pretreated with 10 μM EM20-25 (IC_{50} approximately 20 μM [Fig. 2b]) and infected with VSV-AV1 (MOI of 10). Pretreatment with EM20-25 for 30 min dramatically diminished the resistance of CLL cells to VSV-induced apoptosis (Fig. 3a). By 96 h postinfection, the combination increased cell death more than fivefold compared to either VSV-AV1 or EM20-25 alone (1.1- and 1.4-fold, respectively) (Fig. 3b). Importantly, synergism measured using a CI of 0.5 (see Materials and Methods) was achieved in all seven samples tested ($P < 0.0001$ for comparison to VSV-AV1 treatment alone or $P < 0.001$ for comparison to EM20-25 treatment alone) (Fig. 3c). Induction of apoptosis by VSV-AV1 and EM20-25 in malignant CLL cells was further confirmed by detection of cleaved caspase-3; the level of cleaved caspase-3 was 7- to 10-fold higher in cells treated with both VSV-AV1 and EM20-25 than in cells treated with either agent alone (Fig. 3d). Analysis of VSV-AV1 replication in malignant primary CLL cells by viral protein production (Fig. 3e), viral M mRNA synthesis (Fig. 3f), and virus titer (Fig. 3g) demonstrated that VSV-AV1 replicates in malignant CLL cells and that EM20-25 did not significantly alter viral replication. Together these data demonstrate that VSV-AV1 in combination with EM20-25 synergistically overcomes apoptosis resistance in primary malignant CLL cells without increasing VSV-AV1 replication.

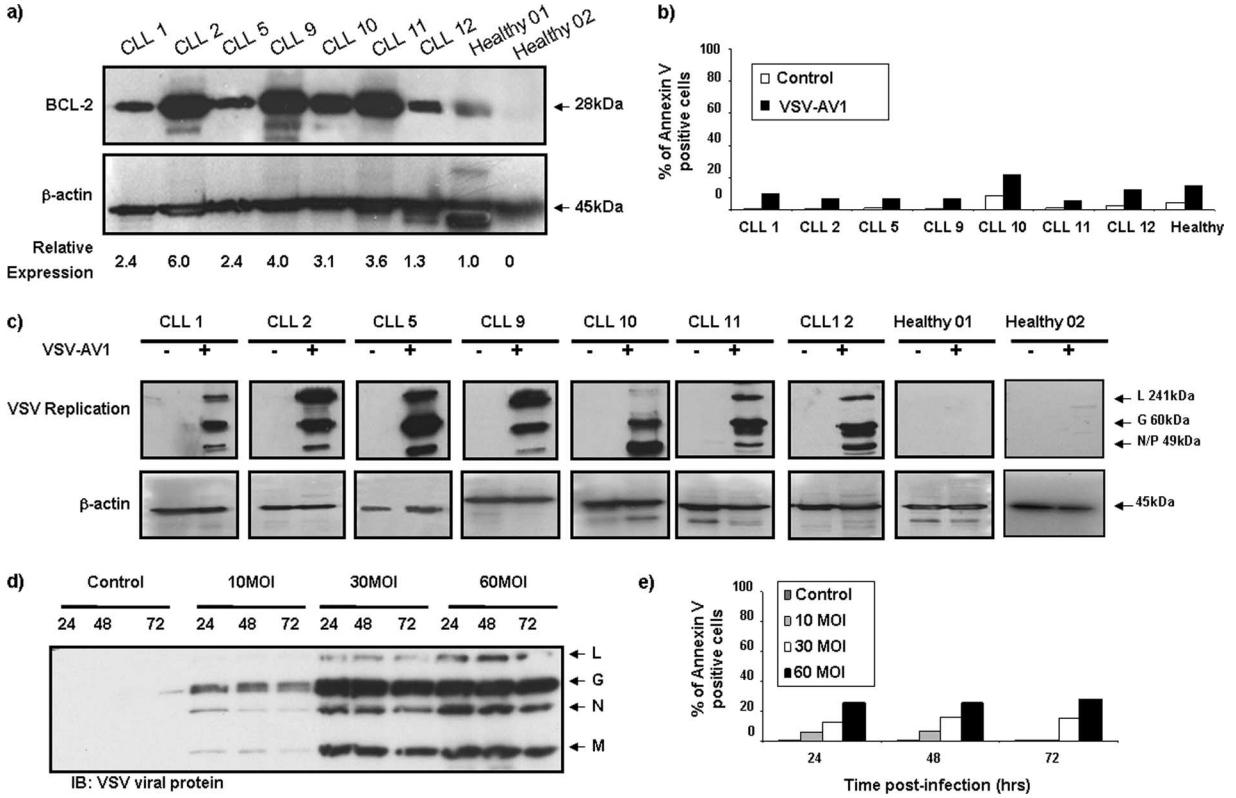

FIG. 1. Primary CLL cells are resistant to VSV-AV1-induced apoptosis. (a) PBMCs were isolated from CLL patients and from two healthy volunteers. Whole-cell extracts were analyzed for BCL-2 protein expression by immunoblotting. The BCL-2 protein expression level was quantified and normalized to the β-actin level. (b) VSV-AV1-induced apoptosis in PBMCs isolated from CLL patients. PBMCs from a healthy volunteer were used as a BCL-2 expression control. At 96 h postinfection, apoptosis was measured using annexin V staining by flow cytometry. Mock-infected cells were used as a control. (c) VSV-AV1 replication in PBMCs isolated from CLL patients and from two healthy volunteers infected with VSV-AV1 (+) or not infected with VSV-AV1 (−) was examined by Western blotting. VSV-AV1 viral protein expression was monitored by Western blot analysis with anti-rabbit VSV antibody. L, large protein; G, glycoprotein; N/P, nucleocapsid. (d and e) PBMCs isolated from a CLL patient (CLL3) were infected with VSV-AV1 at different MOIs (MOIs of 10, 30, and 60). Mock-infected cells were used as a control. (d) VSV viral protein expression was monitored as described above for panel c. The time postinfection (24, 48, and 72 hours after infection) is shown above the lanes. IB, immunoblotting; N, nucleocapsid. (e) VSV-AV1-induced apoptosis in PBMCs from a CLL patient measured by annexin V staining. Mock-infected cells were used as a control.

VSV-AV1 in combination with EM20-25 induces apoptosis through the intrinsic mitochondrial pathway. To further corroborate the data obtained in primary CLL cells, we sought to identify cell lines that expressed BCL-2 protein at levels similar to those in CLL cells. Among 12 B-lymphoma cell lines tested, Karpas-422 and Granta-519 naturally overexpress BCL-2 to levels comparable to those in ex vivo PBMCs from CLL patients (Fig. 4a; also see Fig. 6a). As with CLL cells, both Karpas-422 and Granta-519 cells had similar EM20-25 toxicity levels (IC_{50}s of approximately 20 μM) (Fig. 2b). Karpas-422 cells were treated with EM20-25 (10 μM) for 30 min and then infected with VSV-AV1 at an MOI of 10. The combination led to a threefold increase in VSV-induced apoptosis compared to the effect of virus alone ($P < 0{,}05$), as demonstrated by annexin V-APC staining (Fig. 4b). When examined by the MTT reduction assay, viability of Karpas-422 cells was reduced threefold with the combination, while the loss of viability was only 1.4-fold when Karpas-422 cells were treated with EM20-25 or VSV alone (Fig. 4c). Interestingly, VSV replication was not significantly affected (Fig. 4d), indicating that apoptosis observed with VSV-AV1/EM20-25 was not accompanied by increased VSV replication.

To link BCL-2 overexpression with resistance to VSV-induced apoptosis, a Jurkat T-cell line expressing BCL-2 under the control of doxycycline (DOX) was used (7). In this cell model, a fourfold increase in BCL-2 was detected 24 h after DOX treatment (Fig. 4e). At 48 h after VSV infection, 85% of control Jurkat cells underwent apoptosis, whereas in BCL-2-expressing Jurkat cells, VSV-AV1-induced apoptosis reached a maximum of 40 to 50% ($P < 0.05$) (Fig. 4f). Pretreatment of BCL-2-expressing Jurkat cells with EM20-25 restored VSV-AV1-induced apoptosis to levels similar to those seen in control Jurkat cells (Fig. 4f). Confirming our results with Karpas-422 cells, treatment with EM20-25 did not affect VSV replication in Jurkat cells (control or BCL-2-expressing cells) (Fig. 4g).

We and others previously reported the importance of the mitochondrial apoptotic pathway in VSV-induced oncolysis (22, 50). The loss of mitochondrial transmembrane potential is known to trigger cytochrome *c* release from the mitochondria

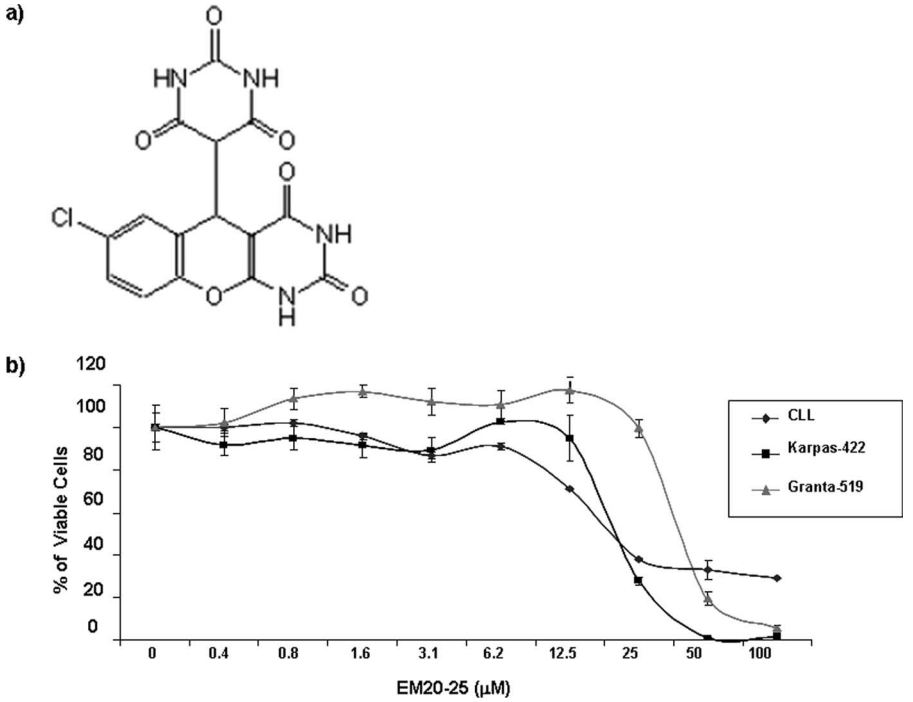

FIG. 2. EM20-25 toxicity. (a) EM20-25 structure. (b) Primary B-CLL cells and Karpas-422 and Granta-519 cells were treated with EM20-25 continuously for 96 h (cell lines) and 5 days (primary cells), and cell viability was quantified by the MTT assay. Each data point represents the mean ± SD (error bar) for quadruplicate wells.

and to promote formation of the apoptosome complex (17, 25). Thus, changes in the mitochondrial membrane potential ($\psi\Delta m$) were examined in Karpas-422 and BCL-2-expressing Jurkat cells. The combination increased mitochondrial membrane depolarization in both Karpas-422 cells (Fig. 5a) and BCL-2-expressing Jurkat cells (Fig. 5b) but not in control Jurkat cells (Fig. 5c), indicating the ability of EM20-25 to enhance VSV-AV1-induced mitochondrial depolarization. Furthermore, cytochrome *c* release in the cytoplasm of Karpas-422 cells was observed only with combination treatment (Fig. 5d). Taken together, our data indicate that inhibition of BCL-2 function using EM20-25 inhibitor augmented VSV-AV1-induced apoptosis through the intrinsic mitochondrial pathway.

Activation of downstream caspases by the combination was assessed in colorimetric caspase activity assays using substrates specific for caspase-3 or caspase-7 and caspase-9. The combined use of VSV-AV1/EM20-25 increased caspase-3/7 and caspase-9 activity 6.3-fold and 4-fold, respectively, while either VSV-AV1 or EM20-25 alone induced caspase-3/7 and caspase-9 activity by 2- to 3-fold and <2-fold ($P < 0.001$), respectively (Fig. 5e). Furthermore, caspase-3 cleavage detected by immunoblotting was 8-fold higher in cells treated with both VSV-AV1/EM20-25 than in cells treated with EM20-25 alone, and caspase-3 cleavage was 2.5-fold higher than in cells treated with VSV-AV1 alone (Fig. 5f). Similar results were also obtained using Granta-519 cells (Fig. 6b to g).

The VSV-AV1/EM20-25 combination induces apoptosis by disruption of BCL-2/BAX interaction. BCL-2 inhibits the mitochondrial apoptotic pathway by preventing oligomerization of the proapoptotic proteins BAX and BAK at the mitochondrial membrane, which in turn blocks cytochrome *c* release, apoptosome formation, and cleavage of caspase-3 (3, 4, 19); thus, disruption of BCL-2 family interactions is an important step in triggering mitochondrial apoptosis. As shown in Fig. 7, combination treatment was able to disrupt BCL-2/BAX interaction in Karpas-422 cells (Fig. 7a and b). Coimmunoprecipitation of BCL-2 followed by immunoblotting with anti-BAX antibody demonstrated the loss of association between BCL-2 and BAX (Fig. 7a and b). An essential step in BAX activation is a conformational change which exposes an epitope at the N terminus of BAX that is occluded in its inactive state (27). To test whether the VSV-AV1/EM20-25 combination directly activated the BAX conformational change, cellular protein extracts prepared after 36 h of treatment were immunoprecipitated with an anti-BAX MAb (6A7) that recognizes the epitope exposed during BAX activation. As shown in Fig. 7b, only cells treated with VSV-AV1/EM20-25 display the prodeath conformation, indicating that the combination promotes conformational changes in BAX that are associated with apoptosis. Importantly, the combination did not significantly alter protein expression of other antiapoptotic BCL-2 family members or the expression of BAX (Fig. 7c), suggesting that changes in BCL-2 levels were not involved in apoptosis induction by the combination. In contrast, EM20-25 alone at 10 μM did not disrupt BAX/BCL-2 interactions, indicating that inhibition of BCL-2 alone is not sufficient to induce apoptosis and that the additional stress signal generated by VSV infection was required to disrupt BCL-2/BAX interaction and trigger downstream apoptosis.

VSV-AV1 and EM20-25 selectively kill $CD5^+$ $CD19^+$ B-CLL cells and spare normal PBMCs. Chemotherapeutic approaches should selectively target cancer cells while leaving

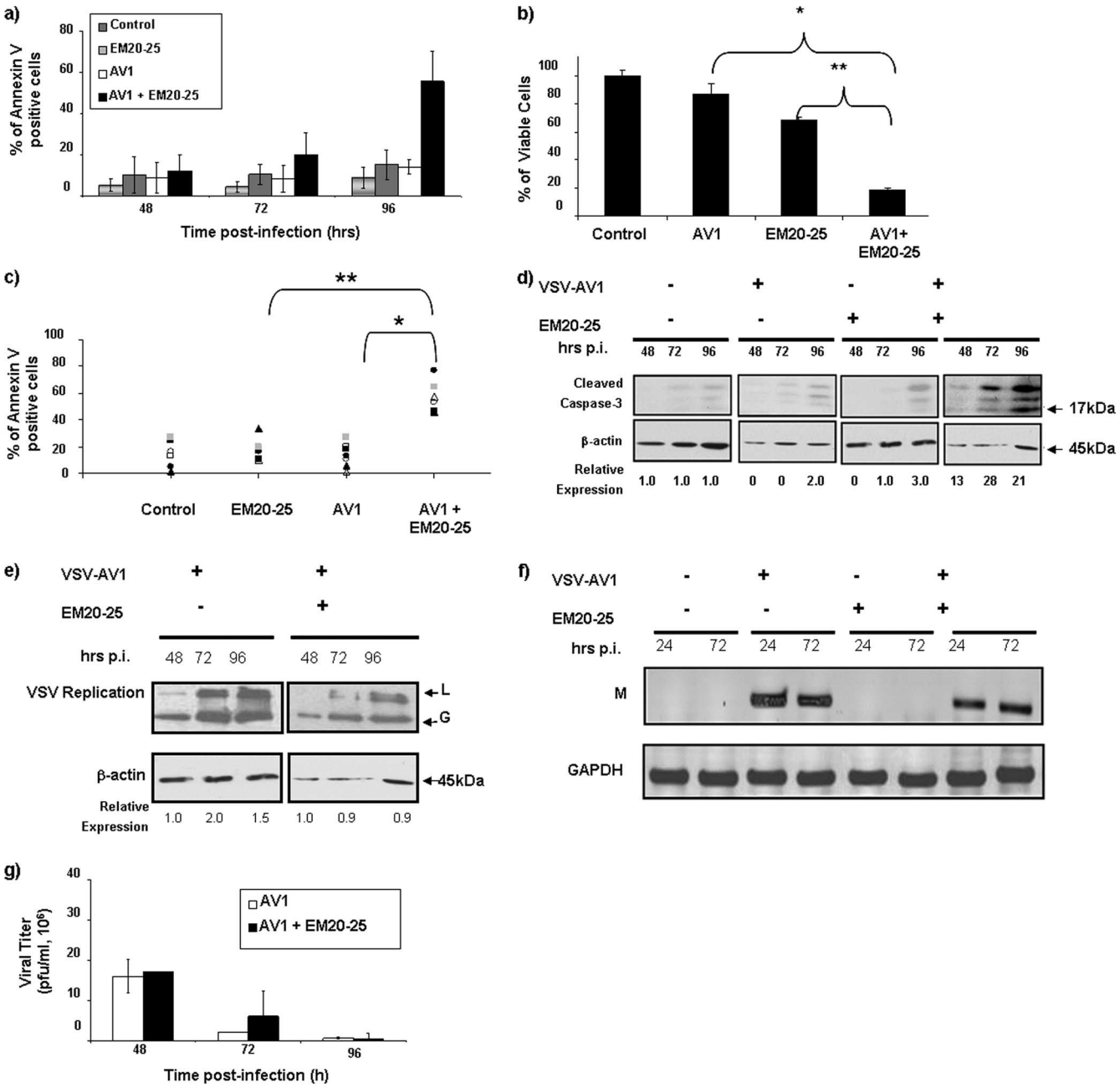

FIG. 3. BCL-2 inhibitor EM20-25 sensitizes ex vivo CLL cells to VSV-AV1 oncolysis. The effect of the combination of VSV-AV1 and EM20-25 (AV1 + EM0-25) in PBMCs isolated from CLL patients is shown. (a) Effect of EM20-25 on VSV-AV1-induced apoptosis. At the indicated times postinfection, apoptosis was measured by annexin V staining. The results are reported as a percentage of viable cells, and the values represent the means ± SDs (error bars) from seven experiments. Noninfected cells were used as a control. (b) VSV-AV1/EM20-25-induced cytotoxicity in PBMCs isolated from a CLL patient (CLL7). At 96 h postinfection, cell viability was assessed by MTT assay. The results are reported as a percentage of viable cells; values represent the means plus SDs (error bars) from quadruplicate experiments. In comparisons of the values, *P* values of <0.0001and <0.0002 are indicated by * and **, respectively. (c) In seven patients (CLL8 to CLL11 and CLL13 to CLL15), the percentage of apoptotic cells in each circumstance was quantified by flow cytometry after annexin V staining. Each symbol represents the percentage of annexin V-positive cells for a particular patient. A paired *t* test was used for comparisons (*P* values of <0.0001and <0.001 are indicated by * and **, respectively). (d) Cleavage of caspase-3 in PBMCs isolated from a CLL patient (CLL5). A representative experiment of five experiments is shown. PBMCs treated (+) with VSV-AV1 or EM20-25 or both and cleaved forms of caspase-3 were detected by Western blotting at the indicated times (in hours) postinfection (p.i.). The expression level of the 17-kDa form, from the cleaved caspase-3 protein, was quantified and normalized to the β-actin level. (e) PBMCs isolated from a CLL patient were treated with VSV-AV1/EM20-25 (+), and viral replication was measured. VSV-AV1 large protein (L) and glycoprotein (G) were detected by Western blotting. (f and g) PBMCs isolated from a CLL patient (CLL9) were treated (+) with VSV-AV1 or EM20-25 or both, and viral replication was measured. GAPDH, glyceraldehyde-3-phosphate dehydrogenase. (f) RT-PCR detection of viral matrix (M) mRNA synthesis; (g) viral titer determined by plaque assay in Vero cells. Values represent the means ± SDs (error bars) from triplicate experiments.

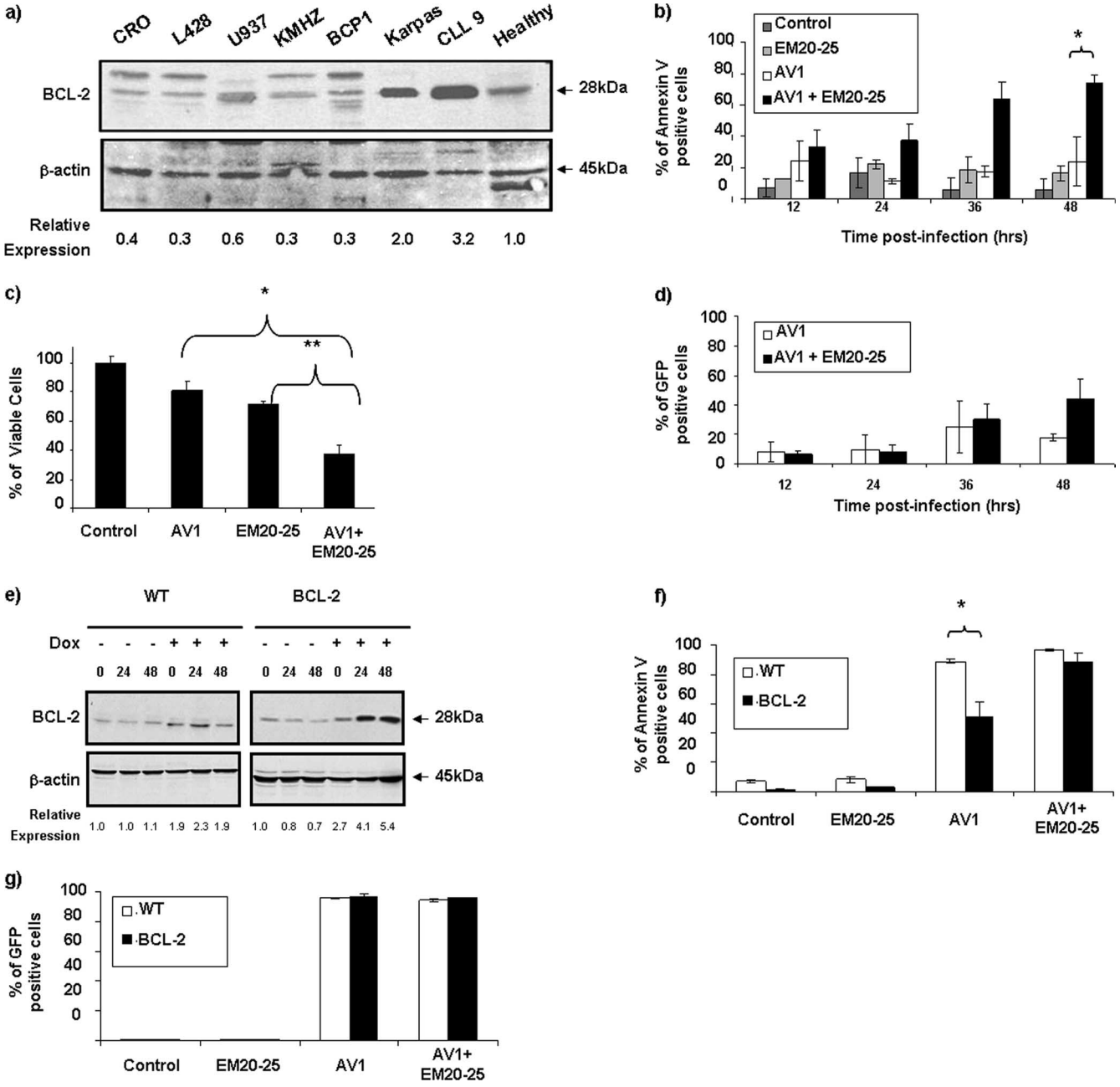

FIG. 4. EM20-25 increases VSV-AV1-induced apoptosis in BCL-2-overexpressing cells. (a) Expression of BCL-2 protein. Different B-cell lines, primary CLL cells, and PBMCs from a healthy donor were examined by immunoblotting for BCL-2 expression. The BCL-2 protein expression level was quantified and normalized to the β-actin level. (b) Kinetics of VSV-AV1/EM20-25-induced apoptosis in Karpas-422 cell line. At the indicated times postinfection (in hours), apoptosis was measured using annexin V staining by flow cytometry; values represent the means ± SDs (error bars) for triplicate experiments. In comparisons of the values, a P value of <0.05 is indicated by an asterisk. Mock-infected cells were used as a control. (c) Karpas-422 cells were cultured in the presence of VSV-AV1/EM20-25 for 48 h, and viability was assessed by MTT assay. The results are reported as a percentage of viable cells; values represent the means plus SDs (error bars) for quadruplicate experiments. In comparisons of the values, P values of <0.005 and <0.002 are indicated by * and **, respectively. (d) Effect of EM20-25 on VSV-AV1-GFP replication in Karpas-422 cells. At the indicated times postinfection, cultures were evaluated for viral replication by flow cytometry. The white bars represent green fluorescent protein (GFP) expression in mock-treated cells, and the black bars represent VSV-AV1-GFP expression in EM20-25-treated cells. (e) Expression of BCL-2 protein in Jurkat cells. Wild-type (WT) Jurkat cells and BCL-2-expressing Jurkat cells were treated with doxycycline (Dox) (+), and BCL-2 protein was detected by Western blotting. The time postinfection (0, 24, and 48 h postinfection) is shown above the lanes. (f) VSV-AV1-GFP-induced apoptosis in control Jurkat (wild type [WT]) and BCL-2-expressing Jurkat cell lines. At 48 h postinfection, apoptosis was measured using annexin V staining by flow cytometry; values represent the means plus SDs (error bars) of triplicate experiments. In comparisons of the values, a P value of < 0.05 is indicated by an asterisk. (g) Effect of EM20-25 on VSV-AV1-GFP replication in control Jurkat (WT) and BCL-2-expressing Jurkat cell lines. At 48 h postinfection, cultures were evaluated for VSV-AV1-GFP replication by flow cytometry.

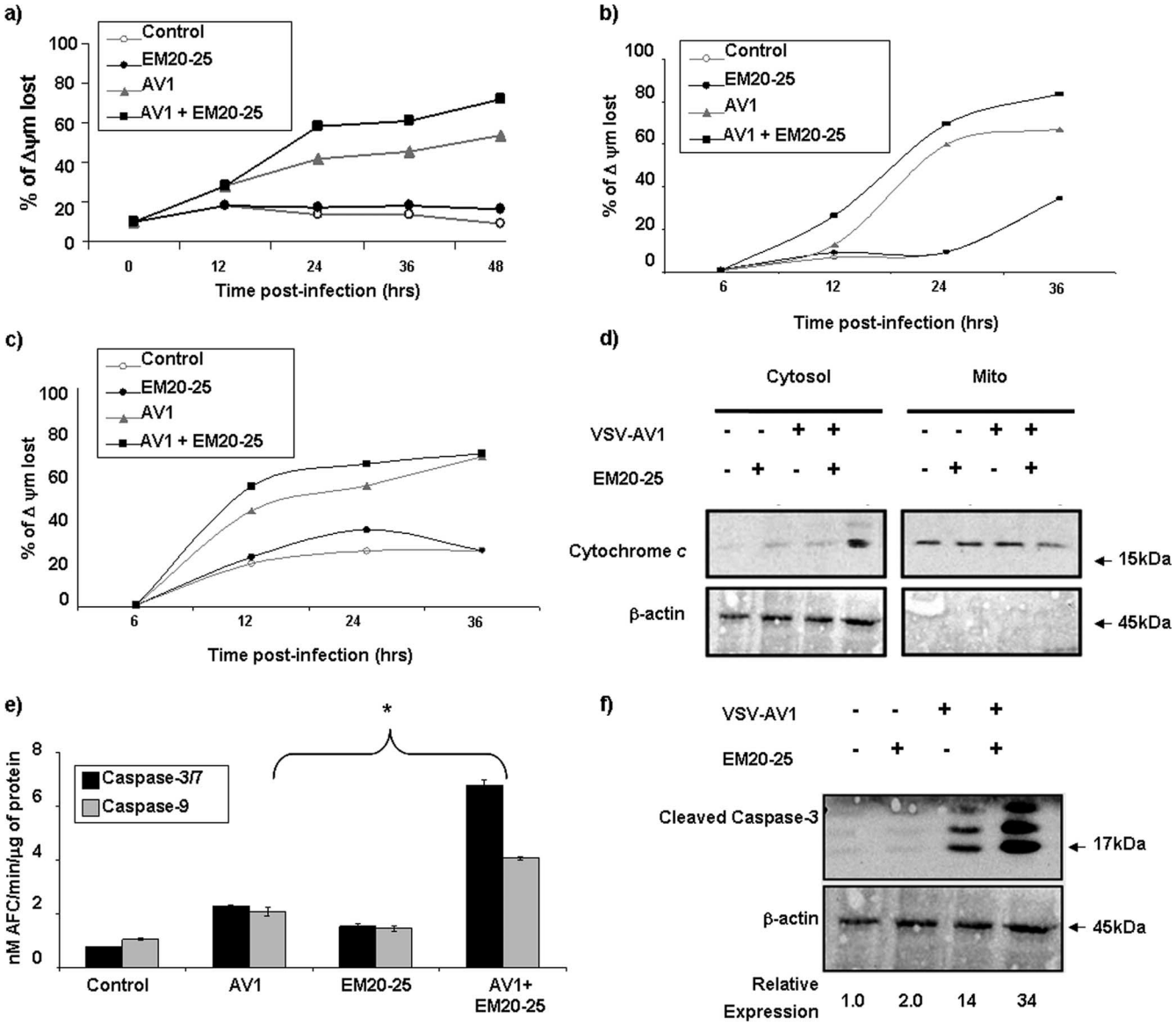

FIG. 5. The combination of VSV-AV1 and EM20-25 induced apoptosis in a mitochondrion-dependent manner. (a) Flow cytometry analysis of Karpas-422 cells following JC-1 staining showed an increase in mitochondrial membrane depolarization after treatment with the VSV-AV1/EM20-25 combination (AV1 + EM20-25). Mock-infected cells were used as a control. The percentage of mitochondrial membrane potential ($\Delta\psi m$) lost is shown. (b) Flow cytometry analysis of BCL-2-expressing Jurkat cells following JC-1 staining showed an increase in mitochondrial membrane depolarization after treatment with VSV-AV1/EM20-25. Mock-infected cells were used as a control. (c) Pretreatment with EM20-25 has no effect in VSV-AV1-induced JC-1 incorporation in control Jurkat cells (wild type [WT]). Mock-infected cells were used as a control. (d) Cytochrome *c* release into the cytosol. Karpas-422 cells were treated (+) with VSV-AV1 or EM20-25 or both. After 36 h postinfection, cells were collected, and cytosolic fractions were prepared as described in Materials and Methods. Cytochrome *c* was detected by Western blotting. Mito, mitochondria. (e) VSV-AV1/EM20-25-induced cleavage of caspases in Karpas-422 cell line. Caspase-3/7 and caspase-9 activities were assayed in cell lysates at 36 h postinfection. Values represent means ± SDs (error bars) for triplicate experiment. In comparisons of the values, a *P* value of <0.001 is indicated by an asterisk. (f) Cleavage of caspase-3. Karpas-422 cells were treated (+) with VSV-AV1 or EM20-25 or both. Cleaved forms of caspase-3 were detected by Western blotting after 36 h postinfection. The expression level of the 17-kDa form, from the cleaved caspase-3 protein, was quantified and normalized to the β-actin level.

normal tissues intact. To examine the target cell selectivity of VSV-AV1/EM20-25 treatment, the CD5 CD19 compartment of PBMCs from a CLL patient was examined for apoptosis induction by annexin V staining. At 96 h postinfection, apoptosis induced by the combination occurred predominantly in the $CD5^+$ $CD19^+$ population (R1) (Fig. 8a), indicating that the combination is specific to leukemic cells; furthermore, EM20-25 did not render the total PBMC population sensitive to VSV-AV1 oncolysis. Indeed, PBMCs isolated from healthy donors were not sensitive to VSV-AV1/EM20-25-mediated apoptosis, as measured by annexin V staining (Fig. 8b). Also, the dose used to treat PBMCs with the combination did not produce significant cytotoxicity in healthy PBMCs (Fig. 8c). Importantly, a direct comparison of healthy PBMCs with primary

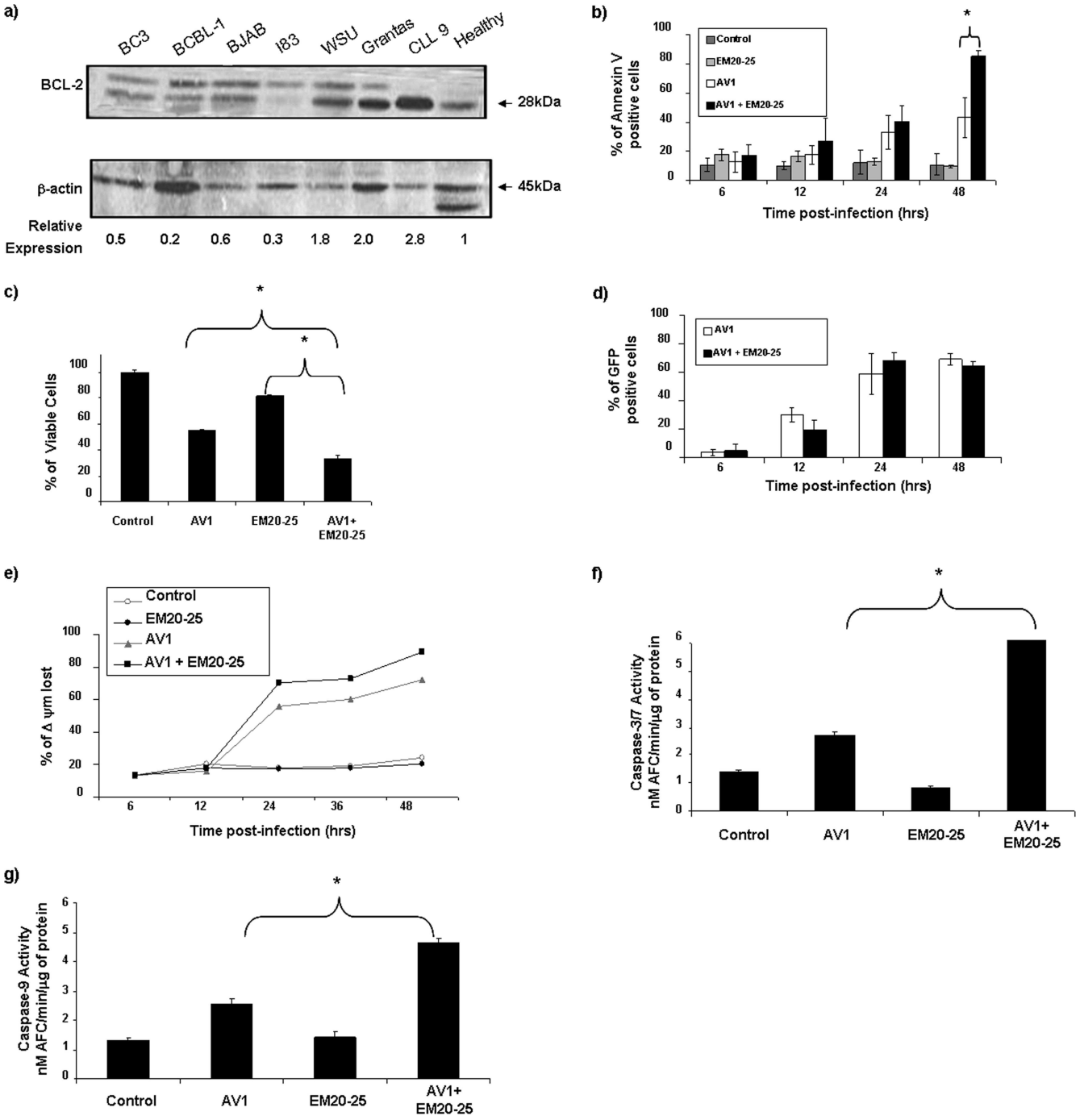

FIG. 6. The resistance of Granta-519 cells to VSV oncolysis is overcome by EM20-25. (a) Expression of BCL-2 protein in six B-lymphoma cell lines compared with ex vivo B-CLL cells (CLL 9) and PBMCs isolated from a healthy donor. Expression of BCL-2 was analyzed in whole-cell extracts by Western blotting with antibody against BCL-2. β-Actin was included as a loading control. The BCL-2 protein expression level was quantified and normalized to the β-actin level. (b) Apoptosis was measured by flow cytometry in Granta-519 cells treated with EM20-25/VSV-Δ51-GFP. Results are presented as bars indicating the percentage of annexin V-positive cells. Mock-infected (control) cells or cells treated with EM20-25 were included as a control. In comparisons of the values, a P value of <0.05 is indicated by an asterisk. (c) Analysis of cytotoxicity by VSV-AV1/EM20-25 in Granta-519 cells. Results are presented as bars indicating the percentage of cell viability. In comparisons of the values, a P value of <0.0001 are indicated by an asterisk. (d) Expression of VSV-Δ51-GFP virus in infected cells was determined by fluorescence-activated cell sorting. Results are presented as a percentage of green fluorescent protein-positive cells in Granta-519 cells. In panels b to d, Data are presented as means ± SDs (error bars). (e) Mitochondrial membrane depolarization (Δ ψm) in response to VSV-AV1/EM20-25 treatment was assessed by flow cytometry using JC-1 staining. Cells were treated with EM20-25/VSV-AV1 prior to JC-1 staining and flow cytometry analysis. Mock-infected cells were used as a control. (f and g) Granta-519 cells were treated as described above. At 36 h postinfection, cells were harvested, and the enzymatic activity of caspase-3/7 (f) and caspase-9 (g) proteases was determined. Results are presented as bars indicating the amount of caspase activity induced compared to the control sample (mock-infected cells). In comparisons of the values, a P value of <0.05 is indicated by an asterisk.

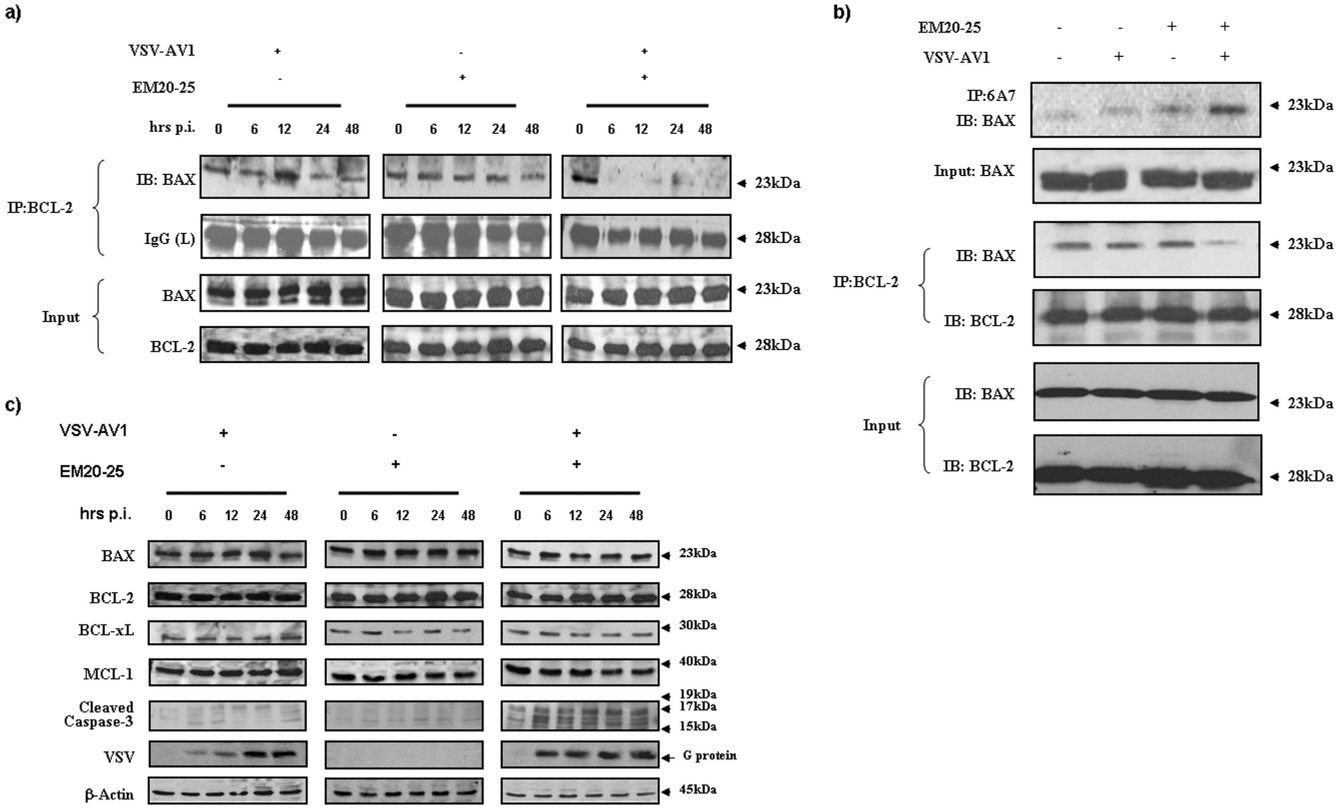

FIG. 7. The combination of VSV-AV1 and EM20-25 induces apoptosis by disruption of BCL-2/BAX interaction. (a) Karpas-422 cells were treated (+) with VSV-AV1 and EM20-25 alone or in combination. After infection (0, 6, 12, 24, and 48 hours postinfection [hrs p.i.]), cells were lysed and BCL-2 was immunoprecipitated. BAX interaction was revealed by immunoblotting (IB) using anti-BAX antibody. IP, immunoprecipitation. IgG, immunoglobulin G; L, light chain. (b) Karpas-422 cells were cultured in the presence of VSV-AV1/EM20-25 for 36 h. Following treatment, cells were lysed in 1% CHAPS lysis buffer and immunoprecipitated with the indicated anti-BCL-2 MAb or anti-BAX (6A7) MAb. Immunoprecipitates were subjected to immunoblotting using anti-BAX antibody. (c) Cells were treated as described above, and pro- and antiapoptotic proteins were detected by immunoblotting. Viral replication (G, glycoprotein) and cleavage of caspase-3 were also monitored by Western blot analysis. β-Actin was added as a loading control.

malignant CLL cells showed that the combination increased the therapeutic index (see Materials and Methods) of the two agents by 19-fold (Fig. 8d) (8, 16, 49).

DISCUSSION

In the present study, we evaluated the therapeutic potential of VSV-AV1 and the BCL-2 inhibitor EM20-25 to induce apoptosis in primary chronic lymphocytic leukemia cells. Primary ex vivo malignant CLL cells were largely resistant to VSV-induced oncolysis, whereas the combination of VSV-AV1 and EM20-25 induced synergistic killing of primary CLL cells, as well as increased VSV-AV1 oncolysis in Karpas-422 and Granta-519 cell lines and disruption of BCL-2/BAX interaction and downstream apoptotic events, such as cytochrome *c* release and caspase-3 cleavage. To our knowledge, this is the first study that demonstrates the value of BCL-2 inhibitors in sensitizing CLL cells to oncolytic virus-induced apoptosis. Our findings support the hypothesis that BCL-2 overexpression creates an apoptosis-resistant phenotype in CLL cells and that blockade of BCL-2 activity sensitizes cells to VSV-AV1-indced oncolysis.

The naturally attenuated VSV-AV1 is a selective oncolytic virus that does not cause significant toxicity in normal human cells. VSV selectivity is achieved by exploiting tumor defects that, while providing cancer cells with growth and survival advantages, compromise the normal innate antiviral program, thus affording a cellular environment that facilitates VSV-AV1 replication and cell killing (9, 32, 37, 53). Although many cell lines are susceptible to viral oncolysis, primary tumors often exhibit significant resistance to oncolytic virus-induced cell death, and this fact has resulted in a search for combination therapeutic strategies that could overcome resistance. In other studies, we demonstrated that VSV-AV1 in combination with histone deacetylase inhibitors enhance oncolytic activity in ex vivo human tumor material and tumor xenograft models, but not in normal primary tissue cultures or peripheral blood mononuclear cells (T. L.-A. Nguyên, H. Abdelbary, M. Arguello, C. Breitbach, S. Leveille, J.-S. Diallo, A. Yasmeen, T. Bismar, D. Kirn, T. Falls, V. Snoulton, B. Vanderhyden, J. Werier, H. Atkins, J. Hiscott, and J. Bell, submitted for publication). Histone deacetylase inhibitors have also been reported to increase herpes simplex virus oncolysis in vivo in glioblastoma models (35). In an elegant study aimed at targeting tumor metastasis, J. Qiao et al. (44) used purified populations of normal autologous T cells to carry VSV to lymph

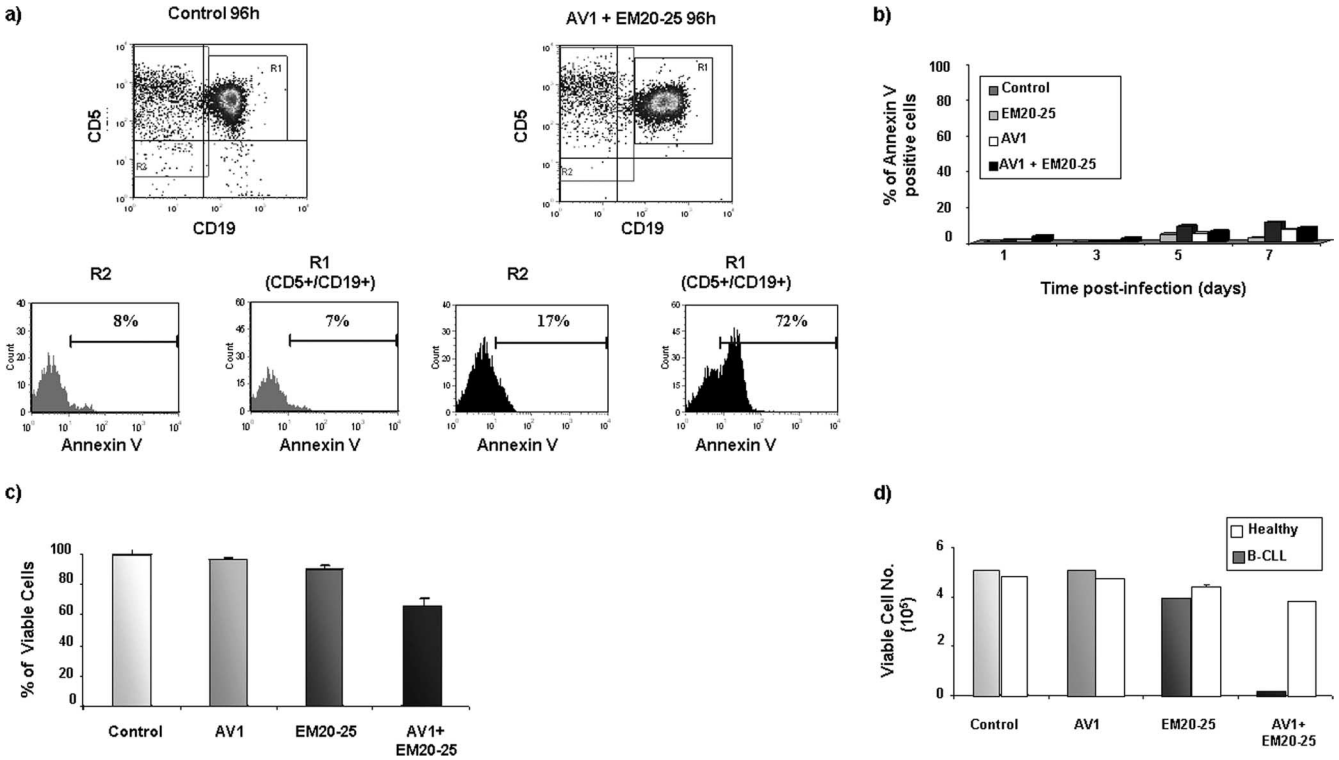

FIG. 8. VSV-AV1 and EM20-25 selectively kill $CD5^+$ $CD19^+$ CLL cells and spare normal PBMCs. (a) Primary PBMCs isolated from CLL patient were treated with the VSV-AV1/EM20-25 (AV1 + EM20-25) combination or not treated with the VSV-AV1/EM20-25 combination (control). At 96 h postinfection, cells were stained for CD5, CD19, and annexin V and analyzed by flow cytometry. Cells positive for both CD5 and CD19 antigens representing B-CLL cells (R1) and non-CLL cells (R2) were electronically gated, and cell death in cells treated with VSV-AV1/EM20-25 compared to the noninfected controls was assessed using flow cytometry. Data are presented as percentages of annexin V-positive cells measured by fluorescence-activated cell sorting in the two different populations, R1 and R2. (b) Effect of EM20-25 on VSV-AV1-induced apoptosis in PBMCs isolated from a healthy volunteer. At the indicated times postinfection, apoptosis was measured by annexin V staining. A representative experiment of three experiments is shown. Mock-infected cells were used as a control. (c) VSV-AV1/EM20-25 did not induce cytotoxicity in PBMCs isolated from a healthy volunteer. At 7 days postinfection, cell viability was assessed by the MTT assay. Results are reported as a percentage of viable cells ± SD; each experiment was performed in quadruplicate. A representative experiment of four experiments is shown. (d) Treatment of primary CLL cells with VSV-AV1/EM20-25 increased the therapeutic index compared to PBMCs from healthy volunteers. At 7 days postinfection, cell viability was assessed by the MTT assay. Results are reported as the mean numbers of viable cells plus SDs (error bars); each experiment was performed in quadruplicate.

nodes and other lymphoid organs. This strategy generated not only metastatic eradication but also antitumor immunity at sites where tumor cell killing occurred (44). Finally, in the present study, we demonstrated that manipulation of the apoptotic pathway can also contribute to increased efficacy of oncolytic virus in CLL cells. Nontoxic doses of EM20-25 were used to restore the ability of CLL cells to induce the intrinsic mitochondrial pathway in response to a stress signal—in this case VSV-AV1. The BCL-2 inhibitor had a synergistic effect, only in combination with VSV-AV1 and only in leukemic cells, thus indicating a safer chemotherapeutic regimen (33, 34, 43, 56). Remarkably, the combination selectively killed the $CD5^+$ $CD19^+$ CLL population, while sparing the normal PBMC population and did not render normal PBMCs susceptible to VSV-induced oncolysis. After VSV-AV1/EM20-25 treatment of Karpas-422 and Granta-519 cell lines and ex vivo primary CLL cells, all cells were eventually killed following combination treatment. However, we cannot rule out the possibility that some primary CLL cells may acquire resistance in vivo. Emergence of a resistant population is dependent on several factors, including the frequency of exposure to virus and drug, the fragility of the leukemic cell population, and time of exposure to the treatment. Further studies are required to investigate the possible emergence of an unresponsive population.

Mitochondrial membrane permeabilization plays a major role in the apoptosis process (48). During apoptosis, the outer mitochondrial membrane becomes permeable to proteins located in the intermembrane space, including cytochrome *c*, which supports formation of the apoptosome, activation of initiator caspase-9, cleavage of the effector caspase-3, and ultimately, processing downstream death substrates (48). Antiapoptotic members of the BCL-2 family, such as BCL-2 and BCL-XL, inhibit protein release from the mitochondria, whereas proapoptotic members, such as BAX and BAK, stimulate this release. Interactions among these pro- and antiapoptotic proteins promote a balance that regulates the fate of the cell (10). VSV induces mitochondrion-dependent apoptosis in a caspase-9/Apaf-1-dependent manner, in part through the viral matrix M protein, which blocks host mRNA export from the nucleus (20–22) by interaction with Rae1/mrnp41 nuclear pore complex proteins (20).

Gaddy and Lyles (24) showed that the inability of the M mu-

tated VSV-AV1 to inhibit host gene expression resulted in the activation of three major initiator caspases—caspase-8, caspase-9, and caspase-12—as well as the executioner caspase-3, suggesting that VSV-AV1 can induce apoptosis via the extrinsic pathway. Furthermore, treatment of cells infected with VSV-AV1 and caspase-8 inhibitor prevented activation of caspase-9 but not caspase-12, indicating that caspase-8 activates caspase-9 (24). This cross talk suggests a mechanism by which VSV-AV1 initially signals through the death receptor pathway, but ultimately both wild-type VSV and VSV-AV1 require the intrinsic mitochondrial pathway to initiate cell death.

BAX represents the convergence point of VSV-mediated cell death, regardless of the VSV strain. Indeed, VSV failed to induce caspase-3 cleavage in BAX/BAK knockout cells, demonstrating a prerequisite for the intrinsic pathway to trigger efficient apoptosis in VSV-infected cells (50). The antiapoptotic protein BCL-2 disrupts the apoptotic program by binding and sequestering proapoptotic BCL-2 family proteins, such as BAX, thus preventing oligomerization, translocation to the mitochondria, and further activation of the intrinsic apoptotic pathway (40). This study provides further evidence of the importance of BCL-2 and the mitochondrial apoptotic pathway in VSV-AV1-induced apoptosis. Mechanistically, current studies focus on the specific proapoptotic proteins inhibited by BCL-2 in CLL cells, as well as the initiator signal used by VSV-AV1 to activate the mitochondrial apoptotic pathway in ex vivo CLL cells.

Overexpression of antiapoptotic BCL-related proteins is a characteristic shared by several malignant diseases (13, 54), especially lymphoid malignancies (18, 28, 54). Downregulation of BCL-2 thus represents an important clinical target in aggressive CLL. A wide array of BCL-2 inhibitors have been synthesized (59), including oligonucleotides, such as G3139 that target BCL-2 mRNA (29, 47), and small molecules, such as EM20-25 (36), ABT-737 (30), HA14-1 (57), and GX015-070 (55), that recognize the surface pocket of BCL-2 or BCL-XL. These molecules disrupt interactions between pro- and antiapoptotic proteins from the BCL-2 family of proteins, leading to tumor regression with single-agent treatment and serve as an important adjuvant in conjunction with conventional therapy (6, 30, 36). Conceivably, inhibition of BCL-2 in malignant cells in combination with conventional chemotherapeutics could translate to a better response (4). Our current understanding of the mechanisms by which BCL-2 controls commitment to cell death provides a strong rationale to augment apoptosis for clinical benefit. The sensitization to VSV-AV1 oncolysis achieved in CLL cells by agents that increase apoptosis thus identifies a promising therapeutic platform for apoptosis-resistant malignancies.

ACKNOWLEDGMENTS

We thank the members of the Molecular Oncology Group, Lady Davis Institute, McGill University, for helpful discussions. We gratefully acknowledge all donors who kindly accepted to participate in this study; without their participation, this study would not be possible.

This research was supported by grants to J.H. from the National Cancer Institute of Canada (NCIC) with funds from the Terry Fox Foundation and the Canadian Institutes of Health Research. V.F.T. is supported by a Studentship from NSERC, S.O. is supported by a Studentship from FRSQ, T.L.-A.N. is supported by a fellowship from FRSQ, and J.H. is a recipient of a CIHR Senior Investigator award.

REFERENCES

1. **Abbott, B. L.** 2006. Chronic lymphocytic leukemia: recent advances in diagnosis and treatment. Oncologist **11:**21–30.
2. **Abbott, B. L.** 2006. Recent advances in chronic lymphocytic leukemia. Cancer Investig. **24:**302–309.
3. **Adams, J. M., and S. Cory.** 2007. Bcl-2-regulated apoptosis: mechanism and therapeutic potential. Curr. Opin. Immunol. **19:**488–496.
4. **Adams, J. M., and S. Cory.** 2007. The Bcl-2 apoptotic switch in cancer development and therapy. Oncogene **26:**1324–1337.
5. **Aghi, M., and R. L. Martuza.** 2005. Oncolytic viral therapies—the clinical experience. Oncogene **24:**7802–7816.
6. **An, J., A. S. Chervin, A. Nie, H. S. Ducoff, and Z. Huang.** 2007. Overcoming the radioresistance of prostate cancer cells with a novel Bcl-2 inhibitor. Oncogene **26:**652–661.
7. **Aouad, S. M., L. Y. Cohen, E. Sharif-Askari, E. K. Haddad, A. Alam, and R. P. Sekaly.** 2004. Caspase-3 is a component of Fas death-inducing signaling complex in lipid rafts and its activity is required for complete caspase-8 activation during Fas-mediated cell death. J. Immunol. **172:**2316–2323.
8. **Banerjee, S., M. Hussain, A. Wang, A. Saliganan, M. Che, D. Bonfil, M. Cher, and F. H. Sarkar.** 2007. In vitro and in vivo molecular evidence for better therapeutic efficacy of ABT-627 and taxotere combination in prostate cancer. Cancer Res. **67:**3818–3826.
9. **Barber, G. N.** 2005. VSV-tumor selective replication and protein translation. Oncogene **24:**7710–7719.
10. **Brenner, C., M. L. Bras, and G. Kroemer.** 2003. Insights into the mitochondrial signaling pathway: what lessons for chemotherapy? J. Clin. Immunol. **23:**73–80.
11. **Cesaire, R., S. Oliere, E. Sharif-Askari, M. Loignon, A. Lezin, S. Olindo, G. Panelatti, M. Kazanji, R. Aloyz, L. Panasci, J. C. Bell, and J. Hiscott.** 2006. Oncolytic activity of vesicular stomatitis virus in primary adult T-cell leukemia. Oncogene **25:**349–358.
12. **Chiorazzi, N., and M. Ferrarini.** 2006. Evolving view of the in-vivo kinetics of chronic lymphocytic leukemia B cells, p. 273–278, 512. American Society of Hematology Education Program Book 2006. Hematology 2006. American Society of Hematology, Washington, DC. http://asheducationbook.hematologylibrary.org/cgi/content/full/2006/1/273.
13. **Choi, J., K. Choi, E. N. Benveniste, Y. S. Hong, J. H. Lee, J. Kim, and K. Park.** 2005. Bcl-2 promotes invasion and lung metastasis by inducing matrix metalloproteinase-2. Cancer Res. **65:**5554–5560.
14. **Chou, T.** 2006. Theoretical basis, experimental design, and computerized simulation of synergism and antagonism in drug combination studies. Pharmacol. Rev. **58:**621–681.
15. **Chou, T. C., and P. Talalay.** 1984. Quantitative analysis of dose-effect relationships: the combined effects of multiple drugs or enzyme inhibitors. Adv. Enzyme Regul. **22:**27–55.
16. **Chun, P. Y., F. Y. Feng, A. M. Scheurer, M. A. Davis, T. S. Lawrence, and M. K. Nyati.** 2006. Synergistic effects of gemcitabine and gefitinib in the treatment of head and neck carcinoma. Cancer Res. **66:**981–988.
17. **Danial, N. N., and S. J. Korsmeyer.** 2004. Cell death: critical control points. Cell **116:**205–219.
18. **Danilov, A. V., A. K. Klein, H. J. Lee, D. V. Baez, and B. T. Huber.** 2005. Differential control of G_0 programme in chronic lymphocytic leukaemia: a novel prognostic factor. Br. J. Haematol. **128:**472–481.
19. **Dlugosz, P. G., L. P. Billen, M. G. Annis, W. Zhu, Z. Zhang, J. Lin, B. Leber, and D. W. Andrews.** 2006. Bcl-2 changes conformation to inhibit Bax oligomerization. EMBO J. **25:**2287–2296.
20. **Faria, P. A., P. Chakraborty, A. Levay, G. N. Barber, H. J. Ezelle, J. Enninga, C. Arana, J. van Deursen, and B. M. Fontoura.** 2005. VSV disrupts the Rae1/mrnp41 mRNA nuclear export pathway. Mol. Cell **17:**93–102.
21. **Fontoura, B. M., P. A. Faria, and D. R. Nussenzveig.** 2005. Viral interactions with the nuclear transport machinery: discovering and disrupting pathways. IUBMB Life **57:**65–72.
22. **Gadaleta, P., X. Perfetti, S. Mersich, and F. Coulombie.** 2005. Early activation of the mitochondrial apoptotic pathway in vesicular stomatitis virus-infected cells. Virus Res. **109:**65–69.
23. **Gaddy, D. F., and D. S. Lyles.** 2007. Oncolytic vesicular stomatitis virus induces apoptosis via signaling through PKR, Fas, and Daxx. J. Virol. **81:**2792–2804.
24. **Gaddy, D. F., and D. S. Lyles.** 2005. Vesicular stomatitis viruses expressing wild-type or mutant M proteins activate apoptosis through distinct pathways. J. Virol. **79:**4170–4179.
25. **Green, D. R., and G. Kroemer.** 2004. The pathophysiology of mitochondrial cell death. Science **305:**626–629.
26. **Guipaud, O., L. Deriano, H. Salin, L. Vallat, L. Sabatier, H. Merle-Beral, and J. Delic.** 2003. B-cell chronic lymphocytic leukaemia: a polymorphic family unified by genomic features. Lancet Oncol. **4:**505–514.
27. **Hsu, Y.-T., and R. J. Youle.** 1997. Nonionic detergents induce dimerization among members of the Bcl-2 family. J. Biol. Chem. **272:**13829–13834.
28. **Irish, J. M., N. Ånensen, R. Hovland, J. Skavland, A. Børresen-Dale, Ø. Bruserud, G. P. Nolan, and B. T. Gjertsen.** 2007. Flt3 Y591 duplication and

Bcl-2 overexpression are detected in acute myeloid leukemia cells with high levels of phosphorylated wild-type p53. Blood **109:**2589–2596.
29. **Kim, R., M. Emi, K. Matsuura, and K. Tanabe.** 2007. Antisense and non-antisense effects of antisense Bcl-2 on multiple roles of Bcl-2 as a chemosensitizer in cancer therapy. Cancer Gene Ther. **14:**1–11.
30. **Kline, M. P., S. V. Rajkumar, M. M. Timm, T. K. Kimlinger, J. L. Haug, J. A. Lust, P. R. Greipp, and S. Kumar.** 2007. ABT-737, an inhibitor of Bcl-2 family proteins, is a potent inducer of apoptosis in multiple myeloma cells. Leukemia **21:**1549–1560.
31. **Letai, A., M. D. Sorcinelli, C. Beard, and S. J. Korsmeyer.** 2004. Antiapoptotic BCL-2 is required for maintenance of a model leukemia. Cancer Cell **6:**241–249.
32. **Lichty, B. D., A. T. Power, D. F. Stojdl, and J. C. Bell.** 2004. Vesicular stomatitis virus: re-inventing the bullet. Trends Mol. Med. **10:**210–216.
33. **Lickliter, J. D., J. Cox, J. McCarron, N. R. Martinez, C. W. Schmidt, H. Lin, M. Nieda, and A. J. Nicol.** 2007. Small-molecule Bcl-2 inhibitors sensitise tumour cells to immune-mediated destruction. Br. J. Cancer **96:**600–608.
34. **Lickliter, J. D., N. J. Wood, L. Johnson, G. McHugh, J. Tan, F. Wood, J. Cox, and N. W. Wickham.** 2003. HA14-1 selectively induces apoptosis in Bcl-2-overexpressing leukemia/lymphoma cells, and enhances cytarabine-induced cell death. Leukemia **17:**2074–2080.
35. **Liu, T.-C., P. Castelo-Branco, S. D. Rabkin, and R. L. Martuza.** 2008. Trichostatin A and oncolytic HSV combination therapy shows enhanced antitumoral and antiangiogenic effects. Mol. Ther. **16:**1041–1047.
36. **Milanesi, E., P. Costantini, A. Gambalunga, R. Colonna, V. Petronilli, A. Cabrelle, S. Semenzato, A. M. Cesura, E. Pinard, and P. Bernardi.** 2006. The mitochondrial effects of small organic ligands of BCL-2: sensitization of BCL-2-overexpressing cells to apoptosis by a pyrimidine-2,4,6-trione derivative. J. Biol. Chem. **281:**10066–10072.
37. **Nakhaei, P., S. Paz, S. Oliere, V. Tumilasci, J. C. Bell, and J. Hiscott.** 2005. Oncolytic virotherapy of cancer with vesicular stomatitis virus. Gene Ther. Mol. Biol. **9:**269–280.
38. Reference deleted.
39. **O'Neill, J., M. Manion, P. Schwartz, and D. M. Hockenbery.** 2004. Promises and challenges of targeting Bcl-2 anti-apoptotic proteins for cancer therapy. Biochim. Biophys. Acta **1705:**43–51.
40. **Packham, G., and F. K. Stevenson.** 2005. Bodyguards and assassins: Bcl-2 family proteins and apoptosis control in chronic lymphocytic leukaemia. Immunology **114:**441–449.
41. **Parato, K. A., D. Senger, P. A. Forsyth, and J. C. Bell.** 2005. Recent progress in the battle between oncolytic viruses and tumours. Nat. Rev. Cancer **5:**965–976.
42. **Pepper, C., A. Thomas, J. Hidalgo de Quintana, S. Davies, T. Hoy, and P. Bentley.** 1999. Pleiotropic drug resistance in B-cell chronic lymphocytic leukaemia—the role of Bcl-2 family dysregulation. Leuk. Res. **23:**1007–1014.
43. **Perez-Galan, P., G. Roue, N. Villamor, E. Campo, and D. Colomer.** 2007. The BH3-mimetic GX15-070 synergizes with bortezomib in mantle cell lymphoma by enhancing Noxa-mediated activation of Bak. Blood **109:**4441–4449.
44. **Qiao, J., T. Kottke, C. Willmon, F. Galivo, P. Wongthida, R. M. Diaz, J. Thompson, P. Ryno, G. N. Barber, J. Chester, P. Selby, K. Harrington, A. Melcher, and R. G. Vile.** 2008. Purging metastases in lymphoid organs using a combination of antigen-nonspecific adoptive T cell therapy, oncolytic virotherapy and immunotherapy. Nat. Med. **14:**37–44.
45. **Rasola, A., and P. Bernardi.** 2007. The mitochondrial permeability transition pore and its involvement in cell death and in disease pathogenesis. Apoptosis **12:**815–833.
46. **Reed, J. C.** 2006. Proapoptotic multidomain Bcl-2/Bax-family proteins: mechanisms, physiological roles, and therapeutic opportunities. Cell Death Differ. **13:**1378–1386.
47. **Rheingold, S. R., M. D. Hogarty, S. M. Blaney, J. A. Zwiebel, C. Sauk-Schubert, R. Chandula, M. D. Krailo, and P. C. Adamson.** 2007. Phase I Trial of G3139, a bcl-2 antisense oligonucleotide, combined with doxorubicin and cyclophosphamide in children with relapsed solid tumors: a Children's Oncology Group Study. J. Clin. Oncol. **25:**1512–1518.
48. **Riedl, S., and G. Salvesen.** 2007. The apoptosome: signalling platform of cell death. Nat. Rev. Mol. Cell Biol. **8:**405–413.
49. **Rots, M. G., D. T. Curielb, W. R. Gerritsenc, and H. J. Haismaa.** 2003. Targeted cancer gene therapy: the flexibility of adenoviral gene therapy vectors. J. Controlled Release **87:**159–165.
50. **Sharif-Askari, E., P. Nakhaei, S. Oliere, V. Tumilasci, E. Hernandez, P. Wilkinson, R. Lin, J. C. Bell, and J. Hiscott.** 2007. Bax-dependent mitochondrial membrane permeabilization enhances IRF3-mediated innate immune response during VSV infection. Virology **365:**20–33.
51. **Sorenson, C. M.** 2004. Bcl-2 family members and disease. Biochim. Biophys. Acta **1644:**169–177.
52. **Stojdl, D. F., B. Lichty, S. Knowles, R. Marius, H. Atkins, N. Sonenberg, and J. C. Bell.** 2000. Exploiting tumor-specific defects in the interferon pathway with a previously unknown oncolytic virus. Nat. Med. **6:**821–825.
53. **Stojdl, D. F., B. D. Lichty, B. R. tenOever, J. M. Paterson, A. T. Power, S. Knowles, R. Marius, J. Reynard, L. Poliquin, H. Atkins, E. G. Brown, R. K. Durbin, J. E. Durbin, J. Hiscott, and J. C. Bell.** 2003. VSV strains with defects in their ability to shutdown innate immunity are potent systemic anti-cancer agents. Cancer Cell **4:**263–275.
54. **Trisciuoglio, D., M. Desideri, L. Ciuffreda, M. Mottolese, D. Ribatti, A. Vacca, M. Del Rosso, L. Marcocci, G. Zupi, and D. Del Bufalo.** 2005. Bcl-2 overexpression in melanoma cells increases tumor progression-associated properties and in vivo tumor growth. J. Cell. Physiol. **205:**414–421.
55. **Trudel, S., Z. Li, J. Rauw, R. Tiedemann, X. Wen, and K. Stewart.** 2007. Preclinical studies of the pan-Bcl inhibitor obatoclax (GX015-070) in multiple myeloma. Blood **109:**5430–5438.
56. **Trudel, S., A. K. Stewart, Z. Li, Y. Shu, S. B. Liang, Y. Trieu, D. Reece, J. Paterson, D. Wang, and X. Y. Wen.** 2007. The Bcl-2 family protein inhibitor, ABT-737, has substantial antimyeloma activity and shows synergistic effect with dexamethasone and melphalan. Clin. Cancer Res. **13:**621–629.
57. **Wlodkowic, D., J. Skommer, and J. Pelkonen.** 2007. Brefeldin A triggers apoptosis associated with mitochondrial breach and enhances HA14-1- and anti-Fas-mediated cell killing in follicular lymphoma cells. Leuk. Res. **31:**1687–1700.
58. **Wollmann, G., M. D. Robek, and A. N. van den Pol.** 2007. Variable deficiencies in the interferon response enhance susceptibility to vesicular stomatitis virus oncolytic actions in glioblastoma cells but not in normal human glial cells. J. Virol. **81:**1479–1491.
59. **Zhai, D., C. Jin, A. C. Satterthwait, and J. C. Reed.** 2006. Comparison of chemical inhibitors of antiapoptotic Bcl-2-family proteins. Cell Death Differ. **13:**1419–1421.